

SOLID-STATE NUCLEAR MAGNETIC RESONANCE SPECTROSCOPY ON SYNTHETIC AMMONIUM/ALUMINUM-SAPONITES*

J. T. KLOPROGGE,^{1,**} J. BREUKELAAR,² A. E. WILSON,² J. W. GEUS,³ AND J. B. H. JANSEN^{1,***}

¹ Department of Geochemistry, Institute of Earth Sciences, University of Utrecht
Budapestlaan 4, P.O. Box 80.021, 3508 TA Utrecht, The Netherlands

² Koninklijke/Shell-Laboratorium Amsterdam (Shell Research B.V.)
P.O. Box 3003, 1003 AA Amsterdam, The Netherlands

³ Department of Inorganic Chemistry, University of Utrecht
P.O. Box 80.083, 3508 TB Utrecht, The Netherlands

Abstract—Ammonium-saponite is hydrothermally grown at temperatures below 300°C from a gel with an overall composition corresponding to $(\text{NH}_4)_{0.6}\text{Mg}_3\text{Al}_{0.6}\text{Si}_{3.4}\text{O}_{10}(\text{OH})_2$. Using ^{27}Al and ^{29}Si solid-state Magic Angle Spinning NMR techniques it is demonstrated that synthetic ammonium-saponites have a rather constant $\text{Si}/\text{Al}^{\text{IV}}$ ratio (≈ 5.5) and an $\text{Al}^{\text{IV}}/\text{Al}^{\text{VI}}$ ratio that varies between 1.5 and 3.8. The above ratios are independent of the synthesis temperature, although an increasing amount of Si, N, and, to a lesser extent, Al are incorporated in an amorphous phase with increasing temperature. ^{27}Al MAS-NMR is unable to differentiate between Al at octahedral and Al^{3+} at interlayer sites. CEC, XRD, and the inability to swell prove the Al^{VI} to be mainly on the interlayer sites. Based on the NH_4^- exchange capacity, X-ray fluorescence, ^{27}Al and ^{29}Si MAS-NMR, it is possible to calculate a relatively accurate structural formula.

Key Words— $^{27}\text{Al}/^{29}\text{Si}$ MAS-NMR, Saponite, Synthesis.

INTRODUCTION

Saponite is a trioctahedral 2:1 phyllosilicate, which is composed of sheets formed by a central octahedral sublayer containing predominantly magnesium ions sharing oxygens with two Si-containing tetrahedral sublayers on both sides. A negative charge is created by isomorphous substitution of Si by aluminum in the tetrahedral sublayers. This negative charge may be compensated by cations such as Na^+ , K^+ , Ca^{2+} in the interlayer separating successive sheets (Figure 1). Aluminum can also substitute for magnesium in the octahedral sublayer following the muscovite substitution: $3\text{Mg} = 2\text{Al} + \text{vacancy}$, without creation of a positive charge. Suquet *et al.* (1981), on the other hand, suggested a substitution of $1\text{Mg} = 1\text{Al}$ creating a positive charge, which compensates a negative charge of the tetrahedral sublayer. Additionally both Al^{3+} and Mg^{2+} can be present as an interlayer cation.

Techniques such as XRD, XRF, IR, or TGA/DTA are unable to determine the precise distribution of the aluminum in saponites. In recent years Magic Angle Spinning Nuclear Magnetic Resonance (MAS-NMR) spectroscopy has proven to be a powerful tool to obtain

such structural information (Sanz and Serratos, 1984; Kinsey *et al.*, 1985; Woessner, 1989).

With ^{29}Si MAS-NMR, it has been demonstrated that the resonance positions (chemical shifts) of silicon atoms are dependent on the branching of the silicon atoms and on the degree of tetrahedral aluminum substitution in the second coordination sphere causing distortion of the tetrahedral sheet resulting in changes in the b-axis parameter (Wilson, 1987). Silicon atoms of phyllosilicates exhibit resonances between -91 and -102 ppm, while each aluminum substitution causes an additional chemical shift downfield of approximately 5–6 ppm (Lippmaa *et al.*, 1980; Kirkpatrick *et al.*, 1985). Therefore, ^{29}Si spectra offer the possibility to establish the extent of the tetrahedral substitution $\text{Si}/(\text{Si} + \text{Al}^{\text{IV}})$ in clay structures.

Magic angle spinning at high field strength makes it possible to observe the $+1/2 \leftrightarrow -1/2$ transition of the ^{27}Al quadrupolar nucleus, which has a spin of $3/2$. In general, octahedral aluminum and tetrahedral aluminum show resonances in the ranges 0–30 ppm and 50–90 ppm, respectively (Wilson, 1987). Due to quadrupolar effects, the determination of the $\text{Al}^{\text{IV}}/\text{Al}^{\text{VI}}$ ratio is less accurate than that of the $\text{Si}/\text{Al}^{\text{IV}}$ ratio.

The aim of this study is to characterize the $\text{Al}^{\text{IV}}/\text{Al}^{\text{VI}}$ and $\text{Si}/\text{Al}^{\text{IV}}$ ratio in ammonium-saponites synthesized by Klopogge (1992) and Klopogge *et al.* (1993) by means of MAS-NMR. Comparison of the b-axis dimensions calculated from the ^{29}Si MAS-NMR data to those determined by XRD will probably give evidence about which substitution occurs in the octahedral sheet. The $\text{Al}^{\text{IV}}/\text{Al}^{\text{VI}}$ and $\text{Si}/\text{Al}^{\text{IV}}$ ratios and the substitution

* This paper is a joint contribution from the Debye Institute, University of Utrecht, The Netherlands, and Shell Research B.V.

** Present address: TNO-Institute of Applied Physics TU Delft, Department of Inorganic Materials Chemistry, P.O. Box 595, 5600 AN Eindhoven, The Netherlands.

*** Present Address: Bowagemi B.V., Prinses Beatrixlaan 20, 3972 AN Driebergen, The Netherlands.

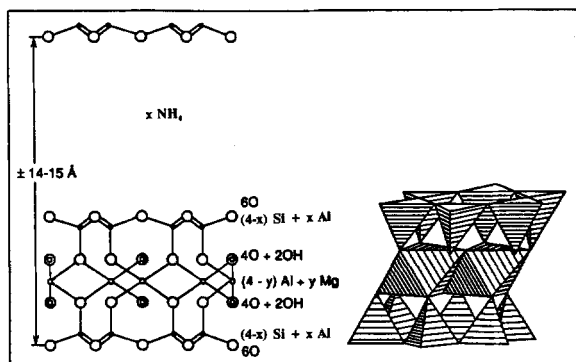


Figure 1. [010] view of a trioctahedral 2:1 phyllosilicate structure.

scheme determine the composition of the tetrahedral and octahedral sheets, which, combined with the chemical data including the CEC, offer the possibility of establishing the structural formulae of the saponites synthesized.

EXPERIMENTAL SECTION

Saponite synthesis

Saponite samples were synthesized using gels prepared of amorphous silica, magnesium acetate, aluminum triisopropylate, and ammonium hydroxide. These gels were hydrothermally treated for 72 h at temperatures between 125° and 280°C and autogeneous water pressure. After cooling, the solid products were washed twice with demineralized water followed by an ion-exchange with a 1 M NH_4Cl solution at room temperature to ensure that all exchangeable sites were occupied by ammonium. The resulting saponites were characterized by means of XRD, XRF, TEM, ICP, and TGA/DTA (Klopprogge, 1992; Klopprogge *et al.*, 1993). Some physical characteristics are given in Table 1. The synthesis temperature was varied between 125°C and 280°C. The initial molar Si/Al ratio in the starting mixture was constant at 5.67 and NH_4^+ was to become the interlayer cation. The small amount (<3% based on XRD data) of corundum in all run products is an artifact caused by the preparation method applied (Klopprogge, 1992; Klopprogge *et al.*, 1993).

Solid-state NMR

^{29}Si solid-state MAS-NMR spectra were recorded at 59.62 MHz on a Bruker CXP-300 spectrometer (magnetic field 7.05 T). ^{27}Al solid-state MAS-NMR spectra were obtained on a Bruker WM-500 spectrometer (130.32 MHz, magnetic field 11.7 T). Both instruments apply a sample spinning rate of approximately 14 kHz. Approximately 4500 Free Induction Decays (FIDs) were accumulated at a repetition time of 12 s (pulse width 3.25 μs) for the ^{29}Si spectra and 3000 FIDs were accumulated at a repetition time of 0.8 s (pulse width

Table 1. Products, Cation Exchange Capacities (CEC), and basal spacings of the saponites examined in this study.

Sample	T (°C)	Products ¹	CEC ² meq/mol	d_{001} (sap) (Å)
HTSAP2a	280	NH_4 -sap + cor	183	12.2
HTSAP2b	240	NH_4 -sap + cor	206	12.3
LTSAP2a	200	NH_4 -sap + cor + am	159	12.3
LTSAP2b	175	NH_4 -sap + cor + am	156	12.3
LTSAP2c	150	NH_4 -sap + cor + am	221	12.3

¹ sap = saponite; cor = corundum; am = amorphous material.

² CEC only based on NH_4 and mol weight of the theoretical saponite composition $(\text{NH}_4)_{0.6}\text{Mg}_3\text{Al}_{0.6}\text{Si}_{3.4}\text{O}_{10}(\text{OH})_2$.

3.0 μs) for the ^{27}Al spectra. Chemical shifts are given in ppm relative to tetramethylsilane (TMS) and $[\text{Al}(\text{H}_2\text{O})_6]^{3+}$, respectively. Upfield shifts are taken to be negative. Due to the fact that the spectra were recorded with a shielded aluminum-free probe, no correction was needed for background signals. Deconvolution of the spectra was obtained by fitting the signals to independent Gaussian lines using a least-squares method. Errors, which mainly depend on the starting conditions, baseline corrections, etc., are estimated to be approximately 5%. These errors, although relevant, are ignored in the calculation of the structural formulae.

RESULTS AND DISCUSSION

The samples were identified by XRD mainly as saponites, with a basal spacing between 12.0 and 12.3 Å, containing 1–3% corundum. At lower synthesis temperatures, a gradually increasing amount of mainly Si-containing amorphous impurity (Klopprogge, 1992; Klopprogge *et al.*, 1993) was observed.

The ^{27}Al NMR spectra show octahedral resonances between 4.5 ppm and 9.0 ppm and tetrahedral resonances between 55 ppm and 70 ppm (an example is given in Figure 2A). Analogous to other clay minerals (Woessner, 1989), the 65.5 ppm and 7 ppm resonances are, therefore, assigned to tetrahedral and octahedral aluminum in the synthetic saponite, respectively. Exchange experiments of ammonium-saponite with $\text{Al}(\text{NO}_3)_3$ have shown that, although a small increase in Al content and minor change in chemical shift is observed, ^{27}Al NMR cannot quantitatively discriminate between aluminum on octahedral sites and on interlayer sites due to overlap of the signals (compare Figures 2A and 2B). Aluminum exchanged beidellite, in comparison, exhibits a resonance of octahedral aluminum (about 3 ppm) together with a recognizable shoulder due to interlayer aluminum (about -3 ppm) (Diddams *et al.*, 1984). The presence of aluminum at interlayer sites is indicated by 1) low exchangeable ammonium, 2) lack of exchangeable Mg^{2+} (Klopprogge, 1992; Klopprogge *et al.*, 1993), and 3) by the failure of

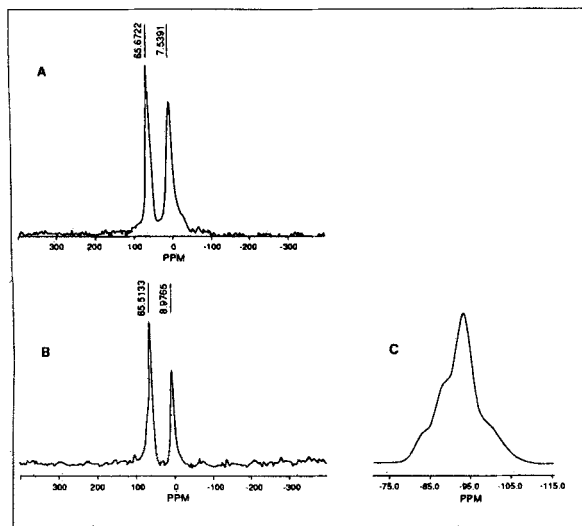


Figure 2. ^{27}Al MAS-NMR spectra of A) NH_4 -saponite, B) Al^{3+} -exchanged saponite, and C) ^{29}Si MAS-NMR spectrum of NH_4 -saponite.

the saponite to swell when suspended in water. The 58.3 ppm resonance is comparable to the tetrahedral resonance at 57.3 ppm of the starting gel and is interpreted to be due to aluminum present in the amorphous phase. The sometimes observed additional resonance at 9.3 ppm (not shown) is assigned to corundum, $\alpha\text{-Al}_2\text{O}_3$ (John *et al.*, 1983), which has only octahedral aluminum in its structure. Due to the fact that aluminum has a quadrupolar nucleus, the $\text{Al}^{\text{IV}} : \text{Al}^{\text{VI}}$ ratio is at low magnetic field less precise than the $\text{Si}/\text{Al}^{\text{IV}}$ ratio based on ^{29}Si NMR. Fortunately, the inaccuracy due to spinning sidebands can be excluded in a high magnetic field (11.7 T) and with a high sample spin frequency (14 kHz). Therefore, the $\text{Al}^{\text{IV}}/\text{Al}^{\text{VI}}$ ratio of the run products and the percentages of total aluminum present in the mentioned phases listed in Table 2 are assumed to be rather accurate after all.

^{29}Si MAS-NMR spectra reveal three resonances of silicon atoms coordinated with one or more next nearest tetrahedral aluminum atoms in the tetrahedral sub-layer of the saponite structure. The resonance with the highest intensity is located at -93.1 ± 0.4 ppm. In addition, a shoulder at -88.5 ± 0.4 ppm and a small shoulder at -83.2 ± 1.2 ppm can be clearly identified. According to results on other synthetic trioctahedral clays by Lipsicas *et al.* (1984), the -93.1 ppm signal is attributed to $\text{Si}(\text{OAl})$, while the two shoulders at -88.5 ppm and -83.2 ppm are assigned to $\text{Si}(\text{1Al})$ and $\text{Si}(\text{2Al})$, respectively (Figure 2C). An additional resonance can be observed at -102 ppm, which is due to amorphous material.

Similar to zeolites, the fraction of tetrahedral $\text{Al}(\text{1Al})$ linkages and $\text{Si}(\text{2Al})$ linkages can be calculated (Lipsicas *et al.*, 1984). If Loewenstein's avoidance principle

Table 2. Aluminum distribution as fractions of total aluminum in the NH_4 -saponite samples based on ^{27}Al MAS-NMR spectra and Si distribution as fractions of total Si and ^{29}Si MAS-NMR line intensities and tetrahedral site distribution parameters of the saponites.

Sample	Saponite			Amorphous	Corundum
	Al^{IV}	Al^{VI}	$\text{Al}^{\text{IV}}:\text{Al}^{\text{VI}}$		
HTSAP2a	0.64	0.17	3.8	0.00	0.19
HTSAP2b	0.61	0.20	3.1	0.00	0.18
LTSAP2a	0.60	0.21	2.9	0.00	0.19
LTSAP2b	0.49	0.14	3.5	0.22	0.15
LTSAP2c	0.32	0.21	1.5	0.36	0.10

Sample	$I_{\text{Si}(\text{OAl})}$	$I_{\text{Si}(\text{1Al})}$	$I_{\text{Si}(\text{2Al})}$	Fraction $\text{Al}(\text{1Al})$	Fraction $\text{Si}(\text{2Al})$	$\text{Si}/\text{Al}^{\text{IV}}$
HTSAP2a	0.494	0.442	0.064	0.05	0.05	5.3
HTSAP2b	0.652	0.160	0.188	0.05	0.18	5.6
LTSAP2a	0.517	0.378	0.105	0.06	0.08	5.1
LTSAP2b	0.590	0.310	0.100	0.04	0.08	5.9
LTSAP2c	0.568	0.332	0.100	0.05	0.08	5.6

Line intensities obtained by fitting the spectra to three independent Gaussian lines using a least-squares method.

holds (Loewenstein, 1954), the fraction of tetrahedral $\text{Al}(\text{1Al})$ linkages should be zero. The tetrahedral aluminum substitution can be calculated directly from the ^{29}Si NMR spectra with the expression (Sanz and Serfatosa, 1984)

$$(\text{Si}/\text{Al})^{\text{IV}} = \frac{\sum_{n=0}^3 I_{\text{Si}(\text{nAl})}}{\sum_{n=0}^3 (n/3) I_{\text{Si}(\text{nAl})}} \quad (1)$$

The values of the experimental ^{29}Si NMR line intensities and site distribution parameters are given in Table 2. An average $\text{Si}/\text{Al}^{\text{IV}}$ ratio of 5.5 is observed for all saponites. The very small fraction of $\text{Al}(\text{1Al})$ linkages indicates that the distribution of aluminum in the tetrahedral sheet is close to statistical (Alma *et al.*, 1984).

The ^{29}Si chemical shifts are systematically related to the total layer charge and the tetrahedral rotation within the a-b plane. The distortion of the tetrahedral sheet is induced by differences in lateral dimensions of the tetrahedral and octahedral sheet. The b-axis dimension of a tetrahedral sheet is systematically influenced by Al^{IV} substitution. The determination of these parameters provide information that cannot be obtained by XRD. The correlation between the chemical shift δ of $\text{Si}(\text{OAl})$ and mean $\text{Si-O}(\text{Si},\text{Al})$ bond angle θ can be represented by

$$\sigma_{\text{Si}(\text{OAl})} (\text{ppm}) = -0.619\theta - 18.7 \text{ ppm} \quad (2)$$

The average deviation α of the Si-O-Si bond angle θ from hexagonal symmetry ($\theta = 109.47^\circ$) enables one to determine the b-axis parameter b_{NMR} with Eq. (3) (Weiss *et al.*, 1987). An α of 0° represents undistorted

Table 3. ^{29}Si MAS-NMR data and structural parameters, based on the Eqs. 2, 3, 4, and 5 of NH_4 -saponites examined in this study.

Sample	$\delta_{\text{Si(OAl)}}^{\circ}$ ppm	$\theta^{\circ}_{\text{obs}}$	$\alpha^{\circ}_{\text{obs}}$	b_{ideal}		b_{NMR}		b_{XRD} (Å)
				(Å) ¹	(Å) ²	(Å) ¹	(Å) ²	
HTSAP2a	-92.6	119.39	9.92	9.267	9.219	9.128	9.081	9.188
HTSAP2b	-92.8	119.71	10.24	9.261	9.217	9.113	9.070	9.174
LTSAP2a	-93.7	121.16	11.69	9.270	9.220	9.078	9.029	9.184
LTSAP2b	-93.0	120.03	10.56	9.254	9.208	9.097	9.052	9.175
LTSAP2c	-93.4	120.68	11.21	9.261	9.212	9.084	9.036	9.175

¹ Based on Guggenheim (1984).² Based on Suquet *et al.* (1981).

tetrahedral sheet and may increase to a theoretical maximum of 30°

$$\cos \alpha = \frac{b_{\text{NMR}}}{b_{\text{ideal}}} \quad (3)$$

with b_{ideal} being defined by Guggenheim (1984) as

$$b(\text{Si}_{1-x}\text{Al}_x) = 9.15 - 0.74x \quad (4)$$

An alternative way to determine b_{ideal} is offered by the relationship formulated by Suquet *et al.* (1981)

$$b_{\text{ideal}} = 9.174 + 0.079 \text{Al}^{\text{IV}} - 0.07 \text{Al}^{\text{VI}} \quad (5)$$

with Al^{IV} measured by ^{29}Si NMR and Al^{VI} with ^{27}Al NMR. The above-mentioned relations provide an estimation of b_{NMR} , following either Guggenheim (1984) (Eq. 4) or Suquet *et al.* (1981) (Eq. 5) from the ^{29}Si NMR data. The latter values can be compared with b_{XRD} from XRD data (Table 3). The b_{NMR} values based on the ^{29}Si and ^{27}Al NMR data obtained with both procedures are considerably smaller than the b -values observed by XRD. Eq. (5), derived by Suquet *et al.* (1981), is based on the assumption of a one-to-one $\text{Mg}^{2+} \leftrightarrow \text{Al}^{3+}$ substitution instead of the normally occurring muscovite substitution $3\text{Mg}^{2+} \leftrightarrow 2\text{Al}^{3+} + 1$ vacancy, which substitution is followed in Eq. (5). Recalculation of α based on b_{XRD} and b_{ideal} (Eq. 4) results in a small correction of Eq. (2):

$$\sigma_{\text{Si(OAl)}} (\text{ppm}) = -0.619\theta - 20.6 \pm 0.4 \text{ ppm} \quad (6)$$

Table 4. Structural formula of the NH_4 -saponite, based on the $\text{Si}/\text{Al}^{\text{IV}}$ and $\text{Al}^{\text{IV}}/\text{Al}^{\text{VI}}$ ratios and CEC values and assuming that all magnesium is incorporated in the saponite structure.

Sample	Unit cell structural formula
HTSAP2a	$(\text{NH}_4)_{0.18}\text{Al}_{0.15}(\text{Mg}_{2.97}\text{Al}_{0.02}\text{vac}_{0.01})$ $(\text{Si}_{3.37}\text{Al}_{0.63})\text{O}_{10}(\text{OH})_2$
HTSAP2b	$(\text{NH}_4)_{0.21}\text{Al}_{0.13}(\text{Mg}_{2.90}\text{Al}_{0.06}\text{vac}_{0.03})$ $(\text{Si}_{3.40}\text{Al}_{0.60})\text{O}_{10}(\text{OH})_2$
LTSAP2a	$(\text{NH}_4)_{0.16}\text{Al}_{0.16}(\text{Mg}_{2.94}\text{Al}_{0.04}\text{vac}_{0.02})$ $(\text{Si}_{3.35}\text{Al}_{0.65})\text{O}_{10}(\text{OH})_2$
LTSAP2b	$(\text{NH}_4)_{0.16}\text{Al}_{0.13}(\text{Mg}_{2.95}\text{Al}_{0.03}\text{vac}_{0.02})$ $(\text{Si}_{3.44}\text{Al}_{0.56})\text{O}_{10}(\text{OH})_2$
LTSAP2c	$(\text{NH}_4)_{0.22}\text{Al}_{0.13}(\text{Mg}_{2.59}\text{Al}_{0.27}\text{vac}_{0.14})$ $(\text{Si}_{3.40}\text{Al}_{0.60})\text{O}_{10}(\text{OH})_2$

whereas recalculation based on b_{ideal} (Eq. 5) results in a slightly larger correction of Eq. (2):

$$\sigma_{\text{Si(OAl)}} (\text{ppm}) = -0.619\theta - 22.2 \pm 0.5 \text{ ppm} \quad (7)$$

Wilson (1987) already indicated that depending on the input data, slightly different relations can be found. The observed values of α are comparable to those calculated for other trioctahedral phyllosilicates with average values between 6° and 10°, but somewhat larger than the values determined from structural refinements (Weiss *et al.*, 1987). The somewhat smaller correction in Eq. (6) supports the use of the muscovite substitution instead of the one Mg to one Al substitution suggested by Suquet *et al.* (1981) in further calculations of the structural formula. This has a considerable influence on the charge of the saponite sheets and, therefore, on the interlayer composition because, with the muscovite substitution, the charge of the tetrahedral sheet is not compensated by the octahedral sheet but only by the interlayer cations.

The $\text{Al}^{\text{IV}}/\text{Al}^{\text{VI}}$ and $\text{Si}/\text{Al}^{\text{IV}}$ ratios based on the ^{27}Al and ^{29}Si NMR spectra enables one to calculate the structural formulae of the synthesized saponites, which are in agreement with the chemical data given by Klopogge (1992) and Klopogge *et al.* (1993). Based on these data and the assumptions that the amount of N determined by the ammonium exchange capacity and all magnesium present in the run products are incorporated in the saponite structure (Table 4), it is possible to calculate the structural formulae.

It is observed that with decreasing synthesis temperature 1) increasing amounts of silicon, aluminum, and nitrogen are found; 2) a positive correlation exists between the contents of amorphous silica and nitrogen; and 3) the amount of exchangeable ammonium decreases. It is suggested that, with decreasing synthesis temperatures, an increasing amount of N is bound to the silica in the amorphous phase, but not as exchangeable ammonium.

CONCLUSIONS

Hydrothermally synthesized saponites exhibit a rather constant $\text{Si}/\text{Al}^{\text{IV}}$ ratio of approximately 5.5 and a $\text{Al}^{\text{IV}}/\text{Al}^{\text{VI}}$ ratio increasing from 1.5 to 3.8 with in-

creasing synthesis temperature, although this trend is not completely clear. In the ^{27}Al MAS-NMR spectra, four resonances can be observed at approximately 65.5 and 7–8 (Al^{IV} and Al^{VI} saponite respectively), 9.3 (Al^{VI} corundum) and 58 (Al^{IV} amorphous material, comparable to the gel). No separate resonance of interlayer Al apart from the octahedral Al^{VI} signal can be observed, although a small shift can be seen. Comparison of the b-axis values from the XRD data and calculations based on the ^{29}Si MAS-NMR data support the muscovite substitution ($3\text{Mg} = 2\text{Al} + \text{vacancy}$) scheme in the octahedral sheet instead of the one-to-one substitution ($1\text{Mg} = 1\text{Al}$) suggested by Suquet *et al.* (1981). Combination of the NMR data ($\text{Al}^{\text{IV}}/\text{Al}^{\text{VI}}$ and $\text{Si}/\text{Al}^{\text{IV}}$ ratios), chemical data such as CEC, and the muscovite substitution enables one to calculate the saponite structural formulae even though other species are present in the solid product.

ACKNOWLEDGMENTS

The authors wish to thank A. de Winter for his help and advice in the laboratory. Paul M. Bertsch and an anonymous reviewer are thanked for their critical reviews of the manuscript.

REFERENCES

- Alma, N. C. M., Hays, G. R., Samoson, A. V., and Lippmaa, E. T. (1984) Characterization of synthetic dioctahedral clays by solid-state silicon-29 and aluminum-27 nuclear magnetic resonance spectrometry: *Anal. Chem.* **56**, 729–733.
- Diddams, P. A., Thomas, J. M., Jones, W., Ballantine, J. A., and Purnell, J. H. (1984) Synthesis, characterization, and catalytic activity of beidellite-montmorillonite layered silicates and their pillared analogues: *J. Chem. Soc., Chem. Comm.* **1984**, 1340–1342.
- Guggenheim, S. (1984) The brittle micas: in *Micas: Reviews in Mineralogy* **13**, S. W. Bailey, ed., Mineralogical Society of America, 61–104.
- John, C. S., Alma, N. C. M., and Hays, G. R. (1983) Characterization of transitional alumina by solid-state magic angle spinning aluminium NMR: *Appl. Catal.* **6**, 341–346.
- Kinsey, R. A., Kirkpatrick, R. J., Hower, J., Smith, K. A., and Oldfield, E. (1985) High resolution aluminum-27 and silicon-29 nuclear magnetic resonance spectroscopic study of layer silicates, including clay minerals: *Amer. Mineral.* **70**, 537–548.
- Kirkpatrick, R. J., Smith, K. A., Schramm, S., Turner, G., and Yang, W.-H. (1985) Solid-state nuclear magnetic resonance spectroscopy of minerals: *Ann. Rev. Earth Planet. Sci.* **13**, 29–47.
- Klopprogge, J. T. (1992) *Pillared Clays: Preparation and Characterization of Clay Minerals and Aluminum-based Pillaring Agents*: Geologica Ultraiectina 91, Ph.D. Thesis, University of Utrecht, The Netherlands.
- Klopprogge, J. T., Breukelaar, J., Jansen, J. B. H., and Geus, J. W. (1993) Development of ammonium-saponites from gels with variable ammonium concentrations and water contents at low temperatures: *Clays & Clay Minerals* **41**, 103–110.
- Lippmaa, E., Mägi, M., Samoson, A., Engelhardt, G., and Grimmer, A.-R. (1980) Structural studies of silicates by solid-state high-resolution ^{29}Si NMR: *J. Amer. Chem. Soc.* **102**, 4889–4893.
- Lipsicas, M., Raythatha, R. H., Pinnavaia, T. J., Johnson, I. D., Giese Jr., R. F., Costanzo, P. M., and Roberts, J. L. (1984) Silicon and aluminium site distributions in 2:1 layered silicate clays: *Nature* **309**, 604–607.
- Loewenstein, W. (1954) The distribution of aluminum in the tetrahedra of silicates and aluminates: *Amer. Mineral.* **39**, 92–96.
- Sanz, J. and Serratos, J. M. (1984) ^{29}Si and ^{27}Al high-resolution MAS-NMR spectra of phyllosilicates: *J. Amer. Chem. Soc.* **106**, 4790–4793.
- Suquet, H., Malard, C., Copin, E., and Pezerat, H. (1981) Variation du parametre b et de la distance basale d_{001} dans une serie de saponites a charge croissante. I. Etats hydrates: *Clay Miner.* **16**, 53–67.
- Weiss, C. A., Altaner, S. P., and Kirkpatrick, R. J. (1987) High resolution ^{29}Si NMR spectroscopy of 2:1 layer silicates: correlation among chemical shift, structural distortions, and chemical variations: *Amer. Mineral.* **72**, 935–942.
- Wilson, M. A. (1987) *NMR Techniques and Applications in Geochemistry and Soil Chemistry*: Pergamon Press, Oxford, 353 pp.
- Woessner, D. E. (1989) Characterization of clay minerals by ^{27}Al nuclear magnetic resonance spectroscopy: *Amer. Mineral.* **74**: 203–215.

(Received 25 January 1993; accepted 21 March 1994; Ms. 2315)